

Weighing Andromeda: Mass estimates of the M 31 galaxy

Souradeep Bhattacharya¹

¹ Inter University Centre for Astronomy and Astrophysics, Ganeshkhind, Post Bag 4, Pune 411007, India

Abstract. Andromeda (M 31) is the nearest giant spiral galaxy to our Milky Way, and, over the past few decades, has been dubbed the most massive member of the Local Group. I explore the evolution of the measured mass of M 31 over the past ~ 80 years, reviewing the different observational and modelling techniques that have developed over time to measure its mass. I discuss the best present-day constraints of the mass of M 31 and the consistency of different techniques.

Keywords. galaxies: individual: M 31

1. Introduction

The Andromeda galaxy (M 31) is the nearest giant spiral galaxy to our Milky Way (MW) and has long been considered its sister galaxy. Together they account for $\sim 90\%$ of the mass of our Local Group (LG; Penarrubia *et. al* 2016). Given its large size and proximity to the MW, M 31 has long been the subject of many path-breaking studies in astronomy, the earliest of which was the first identification of “island universes” beyond the MW (Hubble 1925, 1929). Measured from Cepheid variables to be at a distance of 285 kpc (Hubble 1925), M 31 (along with the Triangulum galaxy, M 33) was the first of many galaxies to be studied, effectively kickstarting the field of Extragalactic Astrophysics.

M 31 was also one of the first galaxies whose mass determination was attempted. Babcock (1939) constructed the rotation curve (RC) of M 31 out to $\sim 100'$ from its center by measuring the radial velocities of its HII regions from spectroscopic observations. Assuming M 31 to be at a distance of 210 kpc[†] and modelling the disc of M 31 as rotating concentric flattened spheroids, Babcock (1939) measured the mass of M 31 as $10.2 \times 10^{10} M_{\odot}$. Babcock (1939) also noted that the nearly constant angular velocity measured at the outer parts of M 31 was opposite to “planetary” type rotation, a problem that would later come to be known as the “missing mass” problem and nearly 30 years later would start the development of Λ CDM cosmology (Ostriker & Peebles 1973).

In this paper, we will go through a near-exhaustive list of mass measurements of M 31. A number of galaxy mass measurement techniques, many of which find their first application to M 31, will be discussed in Section 2. We will then compare the mass estimate of M 31 from different techniques, discuss possible reasons of discrepancies if any, and finally obtain the present-day best mass estimate of M 31 in Section 3.

2. Mass measurements of the Andromeda galaxy

The various mass measurements of M 31 discussed in this paper have been noted in Table 1 along with the original source of the measurement, the technique employed, the distance to M 31 assumed by the original source as well as the enclosed radius within which the mass has been measured (r_{enc} ; calculated assuming the present-day best known distance to

[†] Babcock (1939) attributes this assumed distance to Hubble (1929). However, the distance for M 31 quoted by Hubble (1929) is 275 kpc.

M 31 of 776 kpc; Savino 2022). The various mass measurements are discussed in the ensuing subsections.

2.1. The disc rotation curve and early mass measurements of M 31

Following the first measurement of the M 31 disc RC by Babcock (1939), the same data were modelled as a thin disc by Wyse & Mayall (1942) leading to a mass estimate of $9.5 \times 10^{10} M_{\odot}$ for M 31. These authors had assumed a variable mass-to-light ratio (M/L) as a function of radius in the M 31 disc. Assuming a constant M/L and thin disc for the M 31 RC from Babcock (1939) and additionally also from Mayall (1950), Schwarzschild (1954) measured a mass of $1.4 \times 10^{11} M_{\odot}$ for M 31. At that time, there was an ongoing tension in the measured distance of M 31, summarized in Hubble & Sandage (1953), and thus Schwarzschild (1954) had assumed a distance of 460 kpc for M 31, an average of the contentious distance estimates. With the same RC data and distance but with a slightly different disc mass model, Lohmann (1954) measured a mass of $3.3 \times 10^{11} M_{\odot}$ for M 31. Soon after, van de Hulst, Raimond & van Woerden (1957) reported the first measurement of the HI gas RC of M 31 from their radio observations. The mass of M 31 based on the HI gas RC was reported by Schmidt (1957) to be $3.38 \times 10^{11} M_{\odot}$, similar to that of Lohmann (1954). Brandt (1960) simultaneously modelled the M 31 disc RC as a thin disc from both HII regions (Babcock 1939; Mayall 1950) and the HI gas (van de Hulst, Raimond & van Woerden 1957) to obtain a similar mass of $3.7 \times 10^{11} M_{\odot}$ for M 31. Both Schmidt (1957) and Brandt (1960) utilised the distance modulus measured for M 31 from cepheid variables by Baade & Swope (1955) but made additional different corrections for extinction (see Table 1 for the values). Roberts (1966) obtained the HI gas RC out to ~ 2 deg in M 31 and assuming a distance of 690 kpc (Baade & Swope 1955) and similar model as Brandt (1960), they obtained a mass of $3.1 \times 10^{11} M_{\odot}$ for the galaxy.

Rubin & Ford (1970) utilised an efficient image-tube spectrograph to measure the radial velocities of individual HII regions in M 31 in reasonable time (1–1.5 hr per HII region). They constructed the RC of M 31 from these HII regions and determined a mass of $1.85 \pm 0.1 \times 10^{11} M_{\odot}$ for M 31. While previous authors had generally termed their determined mass as the total (or near total) mass of M 31, Rubin & Ford (1970) had noted that their determined mass was the enclosed mass and that there should be more missing mass in the outskirts of the galaxy, which later became clearer as they and their contemporaries applied their efficient observation techniques to other galaxies (see review by Faber & Gallagher 1979). However, Einasto & Rummel (1970) simultaneously modelled the observed luminosity distribution of stars in M 31 and the RC from HII regions and HI gas to obtain a similar mass of $2 \times 10^{11} M_{\odot}$ for M 31, but showing that no missing mass is required at least within the enclosed radius to reconcile the RC with the luminosity distribution of the galaxy. Similar values of the M 31 mass were computed by Gottesman & Davies (1970), Roberts & Whitehurst (1975) and Emerson (1976), and later by Braun (1991) and even Carignan *et. al* (2006) from their respective HI gas RC measurements, and by Deharving & Pellet (1975) for their RC constructed from HII regions (see Table 1). A distance of 690 kpc (Baade & Swope 1955) to M 31 was generally accepted. These authors all quoted their mass obtained as being the enclosed mass out to their probed radius (see r_{enc} in Table 1).

At this time, bolstered by the suggestion of a massive dark halo required to support disc galaxies (Ostriker & Peebles 1973), alternative methods to measure the mass of galaxies started becoming popular. One of the earliest applied to M 31 was by Hartwick & Sargent (1974) who applied the virial theorem to the globular cluster (GC) population of M 31 (identified by van den Bergh 1969). The GCs only enclosed a small radius in M 31 and they measured a similar mass as other authors did from the RCs (see Table 1). They had assumed a slightly lower distance of M 31 from Sandage & Tammann (1971). During this time, Gunn (1975) utilised the timing argument (Kahn & Woltjer 1959) to simultaneously measure the mass of the MW and M 31,

reporting a very high but uncertain mass of $4 \times 10^{12} M_{\odot}$ for M 31. [Hodge \(1975\)](#) used the radial velocities of two dwarf satellites of M 31, NGC 247 and NGC 185, and applied tidal radius equations to obtain a similarly high and uncertain mass of $6 \times 10^{12} M_{\odot}$ for M 31. [Rood \(1979\)](#) applied the virial theorem to the radial velocities of the six most luminous satellite galaxies of M 31 and mass of $3.38 \times 10^{11} M_{\odot}$ for M 31, an uncertain value but one that is in-line with that measured in the central regions for M 31 from RCs.

Such mass determination methods of M 31 and their development to present days are discussed individually in the ensuing subsections.

2.2. Satellite radial velocity measurements

Given that M 31 satellites occur at larger distances from the galaxy, they are thought to trace the mass of M 31 out to larger radii. The projected mass estimator method introduced by [Bahcall & Tremaine \(1981\)](#) brought an improvement to the viral mass technique used by [Rood \(1979\)](#), determining the mass of M 31 as $\sim 10^{12} M_{\odot}$. The same projected mass estimator method was applied using an additional M 31 satellite by [van den Bergh \(1981\)](#) to find slightly lower masses (see Table 1). Once more M 31 satellites were identified with measured radial velocities and the distance to M 31 was updated to 770 kpc (close to its present day value; [Holland 1998](#)), updated measurements of the mass of M 31 utilising variations of the projected mass estimator were reported (see Table 1) by [Evans & Wilkinson \(2000\)](#) and [Cote et al. \(2000\)](#). Notably, [Evans & Wilkinson \(2000\)](#) also utilised GCs and Planetary Nebulae (PNe) in M 31 to trace its mass. [Evans et al. \(2003\)](#) developed the tracer mass estimator method and applied it to the satellites of M 31 to measure a mass of $1.1 \times 10^{12} M_{\odot}$ for the M 31 galaxy. The latest iteration of this technique was applied by [Watkins, Evans & An \(2010\)](#) to obtain a mass of $\sim 1.4 \times 10^{12} M_{\odot}$ for M 31 out to 300 kpc (well beyond their estimated virial radius of M 31).

2.3. Globular cluster radial velocity measurements

Similar to satellite galaxies, the projected mass estimator method ([Bahcall & Tremaine 1981](#)) was applied to GCs to estimate the mass of M 31 enclosed by these tracers. [van den Bergh \(1981\)](#) measured a mass of $2.4 \pm 0.12 \times 10^{11} M_{\odot}$ for M 31 within ~ 22.8 kpc, similar to that from RCs at this radius. [Evans et al. \(2003\)](#) utilised the tracer mass estimator technique for GCs but now extrapolated out to 100 kpc to find that M 31 has a mass of $1.2 \times 10^{12} M_{\odot}$, consistent with that from applying the same technique to satellite galaxies. With an updated sample of GCs and slightly larger M 31 distance of 780 kpc ([McConnachie et al. 2005](#)), the same technique led to a larger measured mass of $2.4 \times 10^{12} M_{\odot}$ for M 31 by [Galleti et al. \(2006\)](#), with a slightly lower value from [Lee et al. \(2008\)](#). The latest application of the tracer mass estimator technique to GCs by [Veljanoski et al. \(2013\)](#) fetched a slightly lower mass of $1.35 \pm 0.35 \times 10^{12} M_{\odot}$ with the authors stating that the determined mass is highly dependent on the chosen model and assumptions within.

2.4. Mass models of M 31

Similar in spirit to the technique from [Einasto & Rummel \(1970\)](#) but now including a bulge, an adiabatic disc and a cuspy halo component described by a NFW ([Navarro, Frenk & White 1996](#)) halo profile, [Klypin, Zhao & Somerville \(2002\)](#) simultaneously fitted the surface brightness profile of M 31 and its RC measurements from CO and HI gas within ~ 35 kpc. From their mass models, they thus obtained a mass of $1.6 \times 10^{12} M_{\odot}$ for M 31. Similar models by [Geehan et al. \(2006\)](#) and [Seigar, Barth, & Bullock \(2008\)](#), however, led to lower modelled mass values of M 31 (see Table 1), nearly half that of [Klypin, Zhao & Somerville \(2002\)](#). Applying similar mass models to their measured HI RCs out to ~ 40 kpc from the center of

M 31, both [Chemin, Carignan & Foster \(2009\)](#) and [Corbelli et. al \(2010\)](#) find slightly larger masses for M 31 of $10^{12} M_{\odot}$ and $1.3 \times 10^{12} M_{\odot}$ respectively. The value is consistent (see [Table 1](#)) with that of [Tamm et. al \(2012\)](#) who utilised stellar population models to obtain a stellar mass map of M 31 using multi-wavelength photometry of M 31, and modelled the total mass of M 31 similar to [Klypin, Zhao & Somerville \(2002\)](#). [Hayashi & Chiba \(2014\)](#) modelled a prolate halo of M 31 to find a total mass of $\sim 1.82 \times 10^{12} M_{\odot}$ for the galaxy. They however noted that the choice of assumed halo density profile (NFW or otherwise) has strong bearing on the measured mass of M 31.

2.5. Substructure radial velocity measurements

From improvements in wide-field imaging techniques and instrumentation, a number of surveys conducted in the outskirts of M 31 led to the identification of a plethora of substructures in the halo of M 31 (see [McConnachie et. al 2018](#), and references therein). The most prominent among these is the Giant Stream (GS). From their galaxy mass models, [Ibata et. al \(2004\)](#) found that the kinematics of the GS require a total mass inside 125 kpc of $\sim 7.5 \times 10^{11} M_{\odot}$. Similar values were found by both [Fardal et. al \(2006\)](#) and [Dey \(2023\)](#) using a similar technique and GS kinematics out to ~ 125 kpc. Accounting for updated kinematic measurements of the GS out to larger radii and updated surface brightness measurements as constraints for mass models, [Fardal et. al \(2013\)](#) found a virial mass of $\sim 2 \times 10^{12} M_{\odot}$ for M 31. The higher mass is also supported by the mass within ~ 37 kpc determined by [Escala et. al \(2022\)](#) from kinematics of the NE-Shelf substructure of M 31 (see [Table 1](#)).

2.6. Local Group kinematics

The relative motion of galaxies in the LG around its barycenter were utilised by [Courteau & van den Bergh \(1999\)](#) to obtain the mass of the LG. They had assumed M 31 to be 1.5 times as massive as the MW and found that M 31 had a mass of $\sim 1.3 \times 10^{12} M_{\odot}$. With an estimate of the M 31 transverse and radial velocities towards the MW, [van der Marel et. al \(2012\)](#) applied the timing argument ([Kahn & Woltjer 1959](#)) to determine a mass of $\sim 1.5 \times 10^{12} M_{\odot}$ for M 31. A similar value was later determined by [Penarrubia et. al \(2014\)](#) with a slightly lower value when the LMC kinematics ([Penarrubia et. al 2016](#)) are considered (see [Table 1](#)). By balancing mass and momentum in the LG, [Diaz et. al \(2014\)](#) simultaneously determined the total mass of the LG as the mass ratio of the MW and M 31. They also found a similar mass of $\sim 1.7 \times 10^{12} M_{\odot}$ for M 31.

2.7. Cosmological simulations

Over the past decade, a number of large scale cosmological simulations have developed, that are well-constrained to observed scaling relations for massive galaxies (see review by [Vogelsberger et. al 2020](#)). One of the earliest use of cosmological simulations to measure the mass of M 31 was from [Tollerud et. al \(2012\)](#), who actually used the virial theorem to determine the M 31 mass from satellite radial velocities but calculated a correction factor by applying the same technique to a simulated galaxy system and checking the discrepancy. Over time, techniques have developed to identify observed galaxy analogues in such cosmological simulations based on observed properties and thereby inferring unobserved properties from the simulated analogues. [Zhai et. al \(2020\)](#) identified LG analogues in the Millenium simulations based on observed properties of the two galaxies and their mutual orbits. Their M 31 analogues thus identified with a radial in-fall into the MW had a mean mass of $\sim 2.5 \times 10^{12} M_{\odot}$ which the report as the mass of M 31. [Villanueva-Domingo et. al \(2021\)](#) carry out a similar exercise but for the SIMBA and TNG simulations identifying the masses of M 31 analogues given the input positions of the observed M 31 and its three most massive satellites (M 33, M 32, M 110)

as well as their radial velocities (for M 31, tangential velocities are also used as a constrain). A similar mean mass of $\sim 2.2 \times 10^{12} M_{\odot}$ is obtained for the analogues and attributed to M 31. [Patel & Mandel \(2022\)](#) also use a similar approach but identify M 31 analogues in Illustris TNG-dark simulations constrained by the radial and tangential motions of four of its satellites – M 33, NGC 185, NGC 147 & IC 10. They find a mean mass of $\sim 3 \times 10^{12} M_{\odot}$ for the analogues and attribute it to M 31.

2.8. Other techniques

[Sofue \(2015\)](#) combined the disc rotation velocities of M 31 with the radial velocities of its satellites and GCs to construct the grand rotation curve of M 31. They then used mass models for the disc, bulge, and an NFW halo to determine the mass of M 31 to be $\sim 2 \times 10^{12} M_{\odot}$. [Kafle et. al \(2018\)](#) used high-velocity PNe to measure the escape velocity of PNe as a function of radius, while also simultaneously constraining the virial mass and virial radius of M 31. They find a mass of $\sim 8 \times 10^{11} M_{\odot}$ for M 31.

3. Discussion

Figure 1 shows the reported mass of M 31 as a function of publication year. From the lowest measured mass of M 31 from [Wyse & Mayall \(1942\)](#) to the highest value from [Patel & Mandel \(2022\)](#), the measured mass of M 31 has increased by almost 30 times over the span of the past ~ 80 years. The initial mass measurements were actually restricted to that of the luminous disc and inner regions of the galaxy. Probing greater and greater enclosed radius of M 31 (see Table 1) using the variety of techniques discussed in Section 2, coupled with improvements in its measured distance, has resulted in a steady increase of the measured mass of M 31 (see Figure 1). Most measurements of the M 31 total mass over the past ~ 20 years do place its mass within $1\text{--}2 \times 10^{12} M_{\odot}$.

[Benisty et. al \(2022\)](#) find a LG mass of $3.4_{-1.1}^{+1.4} \times 10^{11} M_{\odot}$ from LG analogues in the Illustris TNG simulations using particularly the M 31 tangential velocities as an important criteria in choosing said analogues. The same simulation suite is used by [Patel & Mandel \(2022\)](#) and [Villanueva-Domingo et. al \(2021\)](#) but using different conditions for choosing M 31 analogues to find M 31 masses of ~ 3 & $\sim 2.2 \times 10^{12} M_{\odot}$ respectively, which are then nearly $\sim 88\%$ & $\sim 66\%$ of the mass of the LG. It is thus clear that the mass of M 31 determined using cosmological simulations depends heavily on the choice of priors. These large-scale cosmological simulations have their mean galaxy masses matched to the observed stellar-mass halo-mass relation. This observed relation would require a typical galaxy with the stellar mass of M 31 to have a halo mass of $\sim 10^{13} M_{\odot}$ ([McGaugh 2023](#)). Thus it is unsurprising that, despite including some priors, M 31 analogues in cosmological simulations tend to be on the more massive end (as the typical M 31 mass galaxies in these simulations lie in more massive haloes). Stronger priors may be necessary to obtain a more accurate measurement of the M 31 mass from their simulated analogues. This is especially true given that there is observational evidence that M 31 has undergone a recent major merger ([Bhattacharya et. al 2019a,b, 2021, 2022, 2023; Arnaboldi et. al 2022](#)) consistent with 2–3 Gyr old 1:4 major merger simulations ([Hammer 2018](#)). This is in sharp contrast to that of the MW (see [Bhattacharya et. al 2023](#), for a summary). Considering the merger history in choosing the simulated analogues of M 31 may yield more accurate mass measurements.

The most accurate total mass measurements of M 31 for the time being come from different techniques discussed in Section 2. To reiterate, [Watkins, Evans & An \(2010\)](#) find a near-total mass of M 31 as $\sim 1.4 \times 10^{12} M_{\odot}$ from applying the tracer mass estimator technique to the radial velocities of M 31 satellites (see Sect 2.2). The same technique applied to GCs ([Veljanoski et. al 2013](#)) also yields a similar M 31 mass (see Sect 2.3). The mass models of M 31 constrained to the latest HI RC in the disc and the surface brightness profile also yield

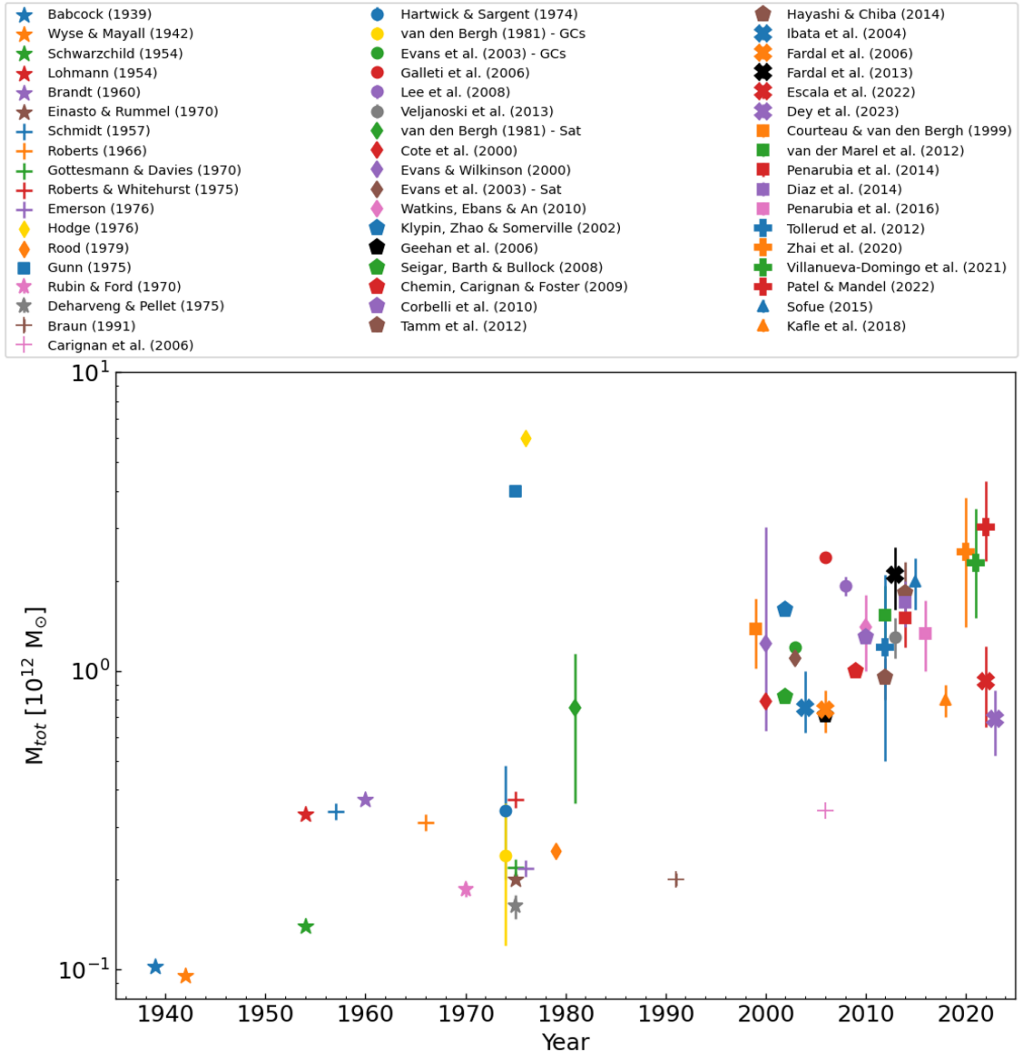


Figure 1. The measured mass of M 31 (in log scale) as a function of publication year. Different symbols refer to different mass measurement techniques that are described in Section 2. Star: RC – HII regions; Narrow plus: RC – HI gas; Diamond: Satellites; Circle – GCs ; Square – LG kinematics; Pentagon – Mass models; Cross – Substructures; Broad plus – simulations; Triangles – others.

a similar mass (Corbelli *et al.* 2010; see Sect 2.4). A mass of $\sim 2 \times 10^{12} M_{\odot}$ is determined from M 31 using models that are consistent with the GS kinematics (Fardal *et al.* 2013; see Sect 2.5). From the timing argument, Penarrubia *et al.* (2016) find the mass of M 31 to be $\sim 1.33 \times 10^{12} M_{\odot}$ (see Sect 2.6). Finally, from the grand RC, Sofue (2015) measure a mass of $\sim 2 \times 10^{12} M_{\odot}$ for M 31.

Considering the mean of the mass of M 31 determined from these works using the aforementioned different techniques, we find that M 31 has a mass of $\sim 1.56 \times 10^{12} M_{\odot}$. There is still a significant margin to improve the mass measurement of M 31 as understood from the previous discussion.

References

- Arnaboldi, M., Bhattacharya, S., Gerhard, O., *et. al* 2022, *A&A*, 666, A109
- Baade, W. & Swope, H. H. 1955, *AJ*, 60, 151
- Babcock, H. W. 1939, Lick Observatory Bulletin, 498, 41
- Bahcall, J. N. & Tremaine, S. 1981, *ApJ*, 244, 805
- Benisty, D., Vasiliev, E., Evans, N. W., *et. al* 2022, *ApJ*, 928, L5
- Bhattacharya, S., Arnaboldi, M., Hartke, J., *et. al* 2019, *A&A*, 624, A132
- Bhattacharya, S., Arnaboldi, M., Caldwell, N., *et. al* 2019, *A&A*, 631, A56
- Bhattacharya, S., Arnaboldi, M., Gerhard, O., *et. al* 2021, *A&A*, 647, A130
- Bhattacharya, S., Arnaboldi, M., Caldwell, N., *et. al* 2022, *MNRAS*, 517, 2343
- Bhattacharya, S., Arnaboldi, M., Hammer, F., *et. al* 2023, arXiv:2304.14151
- Brandt, J. C. 1960, *AJ*, 131, 293
- Braun, R. 1991, *ApJ*, 372, 54
- Carignan, C., Chemin, L., Huchtmeier, W. K., *et. al* 2006, *ApJ*, 641, L109
- Corbelli, E., Lorenzoni, S., Walterbos, R., *et. al* 2010, *A&A*, 511, A89
- Cote, P., Mateo, M., Sargent, W. L. W., *et. al* 2000, *ApJ*, 537, 91
- Courteau, S. & van den Bergh, S. 1999, *AJ*, 118, 337
- Chemin, L., Carignan, C. & Foster, T. 2009, *ApJ*, 705, 1395
- Deharveng, J. & Pellet, A. 1975, *A&A*, 38, 15
- Dey A., Najita, J. R., Kuposov, S. E., *et. al* 2023, *ApJ*, 944, 1
- Diaz, J. D., Kuposov, S. E., Irwin, M., *et. al* 2014, *MNRAS*, 443, 1688
- Einasto J., & Rummel U. 1970, in Becker W., Kontopoulos G. I., eds, Proc. IAU Symp. 38, The Spiral Structure of Our Galaxy. Reidel, Dordrecht, p. 51
- Emerson, D. T. 1976, *MNRAS*, 176, 321
- Escala, I., Gilbert, K. M., Fardal, M. A., *et. al* 2022, *AJ*, 164, 20
- Evans, N. W. & Wilkinson, M. I. 2000, *MNRAS*, 316, 929
- Evans, N. W., Wilkinson, M. I., Perrett, K. M., *et. al* 2003, *ApJ*, 583, 752
- Faber, S. M. & Gallagher, J. S. 1979, *AR&AA*, 17, 135
- Fardal, M. A., Babul, A., Geehan, J. J. *et. al* 2006, *MNRAS*, 366, 1012
- Fardal, M. A., Weinberg, M. D., Babul, A., *et. al* 2013, *MNRAS*, 434, 2779
- Galletti, S., Federici, L., Bellazzini, M. *et. al* 2006, *A&A*, 456, 985
- Geehan, J. J., Fardal, M. A., Babul, A., *et. al* 2006, *MNRAS*, 366, 996
- Gottesman, S. & Davies, R. 1970, *MNRAS*, 149, 263
- Gunn, J. 1975, *Comments Ap. Sp. Phys.*, 6, 7
- Hammer F., Yang Y. B., Wang J. L., *et. al* 2018, *MNRAS*, 475, 2754
- Hartwick, F. & Sargent, W. 1974, *ApJ*, 190, 283
- Hayashi, K. & Chiba, M. 2014, *ApJ*, 789, 62
- Hodge, P. W. 1975, *Bulletin of the American Astronomical Society*, 7, 506
- Hodge P. W., ed. 1992, *Astrophysics and Space Science Library Vol. 176*. Kluwer, Dordrecht
- Holland, S. 1998, *AJ*, 115, 1916
- Hubble, E. P. 1925, *The Observatory*, 48, 139
- Hubble, E. P. 1929, *ApJ*, 69, 103
- Hubble, E. P. & Sandage, A. 1953, *ApJ*, 118, 353
- Ibata, R., Chapman, M., Ferguson, A. M. N., *et. al* 2004, *MNRAS*, 351, 117
- Kafle, P. R., Sharma, S., Lewis, G. F., *et. al* 2018, *MNRAS*, 475, 4043
- Kahn, F. D. & Woltjer, L. 1959, *ApJ*, 130, 705
- Klypin, A., Zhao H. & Somerville R. S. 2010, *ApJ*, 573, 597
- Lee, M. G., Hwang, H. S., Kim, S. C. *et. al* 2008, *ApJ*, 674, 886
- Lohmann, W. 1954, *Zeitschrift für Astrophysik*, 35, 159
- Mateo, M. 1998, *ARA&A*, 36, 435
- Mayall, N. U. 1950, *Publication of the Observatory of the University of Michigan*, 10, 19
- McConnachie, A. W., Irwin, M. J., Ferguson, A. M. N., *et. al* 2005, *MNRAS*, 356, 979
- McConnachie, A. W., Ibata, R., Martin, N., *et. al* 2018, *ApJ*, 868, 55
- McGaugh, S. 2023, arXiv:2305.00858

- Navarro, J. F., Frenk, C. S., & White, S. D. M. 1996, *ApJ*, 462, 563
- Ostriker, J. P., & Peebles, P. J. E. 1973, *ApJ*, 186, 467
- Patel, E. & Mandel, K. S. 2022, arXiv:2211.15928
- Penarrubia, J., Ma, Y. Z., Walker, M. G., *et. al* 2014, *MNRAS*, 443, 2204
- Penarrubia, J., Gomez, F. A., Besla, G., *et. al* 2016, *MNRAS*, 456, L54
- Roberts, M. S. 1966, *ApJ*, 144, 639
- Roberts, M. & Whitehurst, R. 1975, *ApJ*, 201, 327
- Rood, H. 1979, *ApJ*, 232, 699
- Rubin, V. & Ford, W. 1970, *ApJ*, 159, 379
- Sandage, A. & Tammann, G. A. 1971, *ApJ*, 167, 293
- Savino, A., Weisz, D. R., Skillman, E. D., *et. al* 2022, *ApJ*, 938, 101
- Schwarzschild, M. 1954, *AJ*, 59, 273
- Schmidt, M. 1957, Bulletin of the Astronomical Institutes of the Netherlands, 14, 17
- Seigar, M. S., Barth, A. J., & Bullock, J. S. 2008, *MNRAS*, 389, 1911
- Sofue, Y. 2015, *PASJ*, 67, 65
- Tamm, A., Tempel, E., Tenjes, P., *et. al* 2012, *A&A*, 536, A4
- Tollerud, E. J., Beaton, R. L., Geha, M. C., *et. al* 2012, *ApJ*, 752, 45
- van de Hulst, H. C., Raimond, E. & van Woerden, H. 1957, Bulletin of the Astronomical Institutes of the Netherlands, 14, 1
- van den Bergh, S. 1969, *ApJS*, 19, 145
- van den Bergh, S. 1981, *PASP*, 93, 428
- van der Marel, R. P., Fardal, M., Besla, G., *et. al* 2012, *ApJ*, 753, 14
- Veljanoski, J., Ferguson, A. M. N., Mackey, A. D., *et. al* 2013, *ApJL*, 768, 33
- Villanueva-Domingo, P., Villaescusa-Navarro, F., Genel, S., *et. al* 2021, arXiv:2111.14874
- Vogelsberger, M., Marinacci, F., Torrey, P., *et. al* 2020, Nature Reviews Physics, 2, 42
- Watkins, L. L., Evans, N. W. & An, J. H. 2010, *MNRAS*, 406, 264
- Wyse, A. B. & Mayall, N. U. 1942, *ApJ*, 95, 24
- Zhai, M., Guo, Q., Zhao, G., *et. al* 2020, *ApJ*, 890, 27

Table 1. Mass measurements of M 31

Publication	Method	$d_{M\ 31}$ [kpc]	r_{enc} [kpc]	M_{tot} [$10^{12} M_{\odot}$]
Babcock (1939)	RC – HII regions	210	22.8	0.102
Wyse & Mayall (1942)	RC – HII regions	210	22.8	0.095
Schwarzschild (1954)	RC – HII regions	460	22.8	0.14
Lohmann (1954)	RC – HII regions	460	27.3	0.33
Schmidt (1957)	RC – HI gas	630	27.3	0.338
Brandt (1960)	RC – HII regions & HI gas	600	34.2	0.37
Roberts (1966)	RC – HI gas	690	27.3	0.31
Rubin & Ford (1970)	RC – HII regions	690	29.6	0.185 ± 0.01
Einasto & Rummel (1970)	RC – HII regions & HI gas	692	34.2	0.2
Gottesman & Davies (1970)	RC – HI gas	690	34.2	0.22
Hartwick & Sargent (1974)	GCs	667	19.3	0.34 ± 0.14
Deharving & Pellet (1975)	RC – HII regions	690	22.8	0.163 ± 0.015
Roberts & Whitehurst (1975)	RC – HI gas	690	34.2	0.37
Gunn (1975)	LG kinematics	690	–	4
Hodge (1975)	Satellites	690	–	6
Emerson (1976)	RC – HI gas	690	31.2	0.218
Rood (1979)	Satellites	667	–	0.338
Bahcall & Tremaine (1981)	Satellites	667	100	1
van den Bergh (1981)	GCs	667	22.8	0.24 ± 0.12
	Satellites	667	–	0.75 ± 0.39
Braun (1991)	RC – HI gas	690	31.3	0.2 ± 0.01
Courteau & van den Bergh (1999)	LG kinematics	758	–	1.33 ± 0.18
Evans & Wilkinson (2000)	Satellites, GCs & PNe	770	–	$1.23^{+1.8}_{-0.6}$
Cote <i>et. al</i> (2000)	Satellites	780	–	0.79 ± 0.05
Klypin, Zhao & Somerville (2002)	Mass model	770	–	1.6
Evans <i>et. al</i> (2003)	GCs	770	100	1.2
	Satellites	770	–	1.1
Ibata <i>et. al</i> (2004)	Substructure	780	125	$0.75^{+0.25}_{-0.13}$
Carignan <i>et. al</i> (2006)	RC – HI gas	780	35	0.34
Galletti <i>et. al</i> (2006)	GCs	784	–	2.4
Fardal <i>et. al</i> (2006)	Substructure	784	125	0.74 ± 0.12
Geehan <i>et. al</i> (2006)	Mass model	784	–	0.71
Seigar, Barth, & Bullock (2008)	Mass model	784	–	0.82
Lee <i>et. al</i> (2008)	GCs	780	100	$1.92^{+0.14}_{-0.13}$
Chemin, Carignan & Foster (2009)	Mass model	785	–	1
Corbelli <i>et. al</i> (2010)	Mass model	785	–	1.3
Watkins, Evans & An (2010)	Satellites	785	300	1.4 ± 0.4
van der Marel <i>et. al</i> (2012)	LG kinematics	770	–	1.54 ± 0.39
Tamm <i>et. al</i> (2012)	Mass model	785	–	0.95 ± 0.15
Tollerud <i>et. al</i> (2012)	Simulation	785	–	$1.2^{+0.9}_{-0.7}$
Fardal <i>et. al</i> (2013)	Substructure	780	–	$1.99^{+0.52}_{-0.41}$
Veljanoski <i>et. al</i> (2013)	GCs	780	200	1.35 ± 0.35
Diaz <i>et. al</i> (2014)	LG kinematics	780	–	1.7 ± 0.3
Hayashi & Chiba (2014)	Mass model	785	200	$1.82^{+0.49}_{-0.39}$
Penarrubia <i>et. al</i> (2014)	LG kinematics	783	–	1.5 ± 0.3
Sofue (2015)	RC	770	31.3	1.99 ± 0.39
Penarrubia <i>et. al</i> (2016)	LG kinematics	783	–	$1.33^{+0.39}_{-0.33}$
Kaffe <i>et. al</i> (2018)	PNe	780	–	0.8 ± 0.1
Zhai <i>et. al</i> (2020)	Simulation	787	–	$2.5^{+1.3}_{-1.1}$
Villanueva-Domingo <i>et. al</i> (2021)	Simulation	–	–	$2.2^{+1.3}_{-0.8}$
Escala <i>et. al</i> (2022)	Substructure	785	36.6	0.926 ± 0.278
Patel & Mandel (2022)	Simulation	776	–	$3.02^{+1.3}_{-0.69}$
Dey (2023)	Substructure	785	125	$0.63^{+0.2}_{-0.13}$

Notes: Column 1: Source publication; Column 2: Method utilised for mass measurement; Column 3: Adopted distance to M 31 in source publication; Column 4: Radius within which enclosed mass has been measured, assuming present day best measured distance of 776 kpc (Savino 2022). The radius is not noted if the method, either directly or indirectly, measures the total mass of M 31.; Column 5: Mass of M 31, as reported.